DMD Fast Forward. Published on August 25, 2020 as DOI: 10.1124/dmd.120.000156
This article has not been copyedited and formatted. The final version may differ from this version.

Title Page

Successful prediction of PET-imaged metformin hepatic uptake clearance in humans using the quantitative proteomics-informed relative expression factor approach

Madhav Sachar[1], Vineet Kumar[1], Lars C. Gormsen[2], Ole Lajord Munk[2] and Jashvant D. Unadkat[1]

[1]Department of Pharmaceutics, University of Washington, Seattle, P.O. Box 357610, WA 98195

[2]Department of Nuclear Medicine & PET Center, Aarhus University Hospital, Palle Juul-Jensens Boulevard 165 , DK 8200 Aarhus N, Denmark

DMD Fast Forward. Published on August 25, 2020 as DOI: 10.1124/dmd.120.000156
This article has not been copyedited and formatted. The final version may differ from this version.

Running Title: IVIVE of metformin hepatic uptake clearance

Corresponding Author: Dr. Jashvant D. Unadkat

Department of Pharmaceutics, Box 357610, University of Washington, Seattle, WA 98195

Telephone: (206) 543-9434, Fax: (206) 543-3204

E-mail: jash@uw.edu

Figures : 4

References: 34

Words in Abstract: 246 (250)

Words in Significance: 55 (80)

Words in Introduction: 566 (750)

Words in Discussion: 890 (1500)

ABBERIVIATONS:

CL, Clearance; IVIVE,*in vitro* to *in vivo* extrapolation; PHH, plated hepatocytes;REF, relative expression factor; DPBS, Dulbecco's phosphate-buffered saline; DTT, dithiothreitol; IAA, iodoacetamide; $CL_{h,s,in}$, hepatic sinusoidal uptake clearance; CL_{int}, Intrinsic clearance; $CL_{int,in\ vitro}$, intrinsic *in vitro* uptake clearance; REF, relative expression factor; MGPGL, mg of protein content per gram of liver tissue ;fu, fraction unbound; WSHM, well-stirred model

DMD Fast Forward. Published on August 25, 2020 as DOI: 10.1124/dmd.120.000156
This article has not been copyedited and formatted. The final version may differ from this version.

ABSTRACT

Predicting transporter-mediated *in vivo* hepatic drug clearance (CL) from *in vitro* data (IVIVE) is important in drug development to estimate first in human dose and the impact of drug interactions and pharmacogenetics on hepatic drug CL. For IVIVE, one can use human hepatocytes and the traditional MGPGL (i.e. mg of protein content per gram of liver tissue) approach. However, this approach has been found to consistently under-predict the observed *in vivo* hepatic drug CL. Therefore, we hypothesized that using transporter-expressing cells and the relative expression factor (REF), determined using targeted quantitative proteomics, will accurately predict *in vivo* hepatic CL of drugs. We have successfully tested this hypothesis in rats with rosuvastatin, which is transported by hepatic OATPs. Here we tested this hypothesis for another drug and another transporter, namely OCT1- mediated hepatic distributional CL of metformin. First, we estimated the *in vivo* metformin hepatic sinusoidal uptake CL ($CL_{h,s,in}$) of metformin by reanalysis of previously published human positron emission tomography imaging data. Next, using the REF approach, we predicted the *in vivo* metformin $CL_{h,s,in}$ using OCT1-transporter expressing HEK293 cells or plated human hepatocytes. Finally, we compared this REF-based prediction with that using the MGPGL approach. The REF approach accurately predicted the *in vivo* metformin hepatic $CL_{h,s,in}$ while the MGPGL approach considerably under-predicted the *in vivo* metformin $CL_{h,s,in}$. Based on these and previously published data the REF approach appears to be superior to the MGPGL approach for a diverse set of drugs transported by different transporters.

DMD Fast Forward. Published on August 25, 2020 as DOI: 10.1124/dmd.120.000156
This article has not been copyedited and formatted. The final version may differ from this version.

Significance

This study is the first to use OCT1-expressing cells and plated hepatocytes to compare proteomics-informed REF approach with the traditional MGPGL approach to predict hepatic uptake CL of metformin in humans. The plasma membrane abundance corrected proteomics-informed REF approach accurately predicted the PET-imaged metformin hepatic uptake CL, whereas the MGPGL approach consistently underpredicted this CL.

DMD Fast Forward. Published on August 25, 2020 as DOI: 10.1124/dmd.120.000156
This article has not been copyedited and formatted. The final version may differ from this version.

Keywords: *in vitro-in vivo* extrapolation; Predictions; metformin; quantitative proteomics; OCT1, hepatic uptake clearance

DMD Fast Forward. Published on August 25, 2020 as DOI: 10.1124/dmd.120.000156
This article has not been copyedited and formatted. The final version may differ from this version.

INTRODUCTION

Predicting transporter-mediated *in vivo* clearance of drugs from *in vitro* data (IVIVE) is important in drug development to estimate first in human dose and inter-individual variability in drug clearance (CL) due to drug interactions and pharmacogenetics. For IVIVE of hepatic metabolic CL of a drug, the relative activity factor (RAF) (with or without a probe drug) is traditionally used. When used without a probe drug, this approach scales the *in vitro* intrinsic metabolic CL of the drug to that *in vivo* using hepatocellularity or mg of protein microsomal protein yield per gram of liver tissue (MGPGL) (Obach et al., 1997; Andersson et al., 2001). When used with a probe drug, the probe drug must selectively measure the intrinsic CL (CL_{int}) of drug by a single enzyme. An alternative approach, the relative expression factor (Rostami-Hodjegan and Tucker, 2007; Soars et al., 2007; Rowland et al., 2011), is used where *in vitro* metabolic CL_{int} of the drug (e.g. in recombinant enzymes) is scaled to that *in vivo* using the ratio of the abundance of the enzyme *in vivo* (e.g. hepatic tissue) to that *in vitro* (e.g. in recombinant enzymes).

Although using RAF for IVIVE of metabolic CL has been successful (Rostami-Hodjegan and Tucker, 2007; Soars et al., 2007; Rowland et al., 2011), predicting transport-mediated CL using this approach results in under-estimation of the observed in vivo CL of the drug (Jones et al., 2012). In addition, the magnitude of this mis-prediction is not uniform across drugs (Jones et al., 2012). Therefore, generalization across drugs cannot be made through the use of a “common” empirical scaling factor. Moreover, because the RAF

DMD Fast Forward. Published on August 25, 2020 as DOI: 10.1124/dmd.120.000156
This article has not been copyedited and formatted. The final version may differ from this version.

requires selective probe substrate and primary human cells (e.g. hepatocytes) this approach cannot be used where selective transporter probe substrates are not available (e.g. OATP substrates) or when primary cells from the organ of interest are not available or validated (e.g. blood-brain endothelial cells/kidney epithelial cells). Therefore, we have hypothesized that the REF approach, coupled with quantitative targeted proteomics, can overcome many of these problems and be used for accurate IVIVE of transporter-mediated CL of drugs. However, like any other approach, the accuracy of REF-based predictions needs to be verified. Indeed, we along with others have shown that this approach can be used to successfully predict *in vivo* transporter mediated CL (Bosgra et al., 2014; Vildhede et al., 2016; Ishida et al., 2018; Kumar et al., 2018) and hepatic concentrations of rosuvastatin (an OATP substrate) obtained through positron emission tomography (PET) imaging (Bosgra et al., 2014; Vildhede et al., 2016; Ishida et al., 2018; Kumar et al., 2018). But, this success needs to be tested with other drugs transported by other transporters such as metformin which is transported into the liver by OCT1 and possibly by OCT3 and THTR2 (Liang et al., 2015; Pakkir Maideen et al., 2017). Therefore, we first estimated the *in vivo* hepatic sinusoidal uptake CL ($CL_{h,s,in}$) of [^{11}C]-metformin by reanalysis of previously published PET imaging data (Gormsen et al., 2016). This reanalysis was conducted to correct for hepatic blood [^{11}C]-metformin content not conducted in that publication. Next, using the REF approach, we predicted the *in vivo* metformin $CL_{h,s,in}$ using transporter expressing cells and plated human hepatocytes (PHH). These predictions were compared with that obtained using the MGPGL approach (i.e. RAF without probe drug). Our prediction of the *in vivo* metformin $CL_{h,s,in}$ was considered a success if it fell within 2-fold of the observed value.

DMD Fast Forward. Published on August 25, 2020 as DOI: 10.1124/dmd.120.000156
This article has not been copyedited and formatted. The final version may differ from this version.

MATERIALS AND METHODS

Chemicals and Reagents

Specific synthetic peptides and corresponding stable labeled peptides for OCT1, Na^+-K^+ ATPase and calreticulin were purchased form New England Peptides (Boston, MA). Bicinchoninic acid assay (BCA) kit, dithiothreitol (DTT), iodoacetamide (IAA), mass spectrometry grade trypsin, pierce cell surface protein isolation kit, HPLC-grade acetonitrile, Dulbecco's phosphate-buffered saline (DPBS), Dulbecco's modified Eagles' medium (DMEM) high glucose medium were purchased form Thermo Fisher Scientific (Rockford, IL). Metformin (hydrochloride salt), thiamine (hydrochloride salt), quinidine, potassium chloride, magnesium sulphate, D-glucose, HEPES, sodium chloride, sodium bicarbonate, calcium chloride dipotassium phosphate and formic acid were purchased from Sigma-Aldrich (St. Louis, MO). [^{14}C]-metformin hydrochloride (114 mCi/mmol) was obtained from Moravek Biochemicals, Inc. (Brea, CA). Collagen-coated 24-well plates were purchased from Corning (Kennebunk, ME). Human hepatocyte thaw medium, INVITROGRO HI medium, INVITROGRO CP medium and TORPEDO antibiotic mix as well as cryopreserved human hepatocytes (PHH) were generously provided by BioIVT (Westbury, NY). OCT1-HEK293 cells were generously provided by SOLVO Biotechnology (Hungary).

DMD Fast Forward. Published on August 25, 2020 as DOI: 10.1124/dmd.120.000156
This article has not been copyedited and formatted. The final version may differ from this version.

Determination of metformin uptake CL_{int} into OCT1-HEK293 cells and human hepatocytes (PHH)

OCT1-HEK293 cells were grown in T-75 cm2 flasks with 20 mL with high glucose DMEM medium supplemented with 10% fetal bovine serum, 2 mM L-glutamine, 100 IU/mL penicillin, and 100 mg/mL streptomycin. Media was changed daily and cells were kept in humidified incubator with 5% carbon dioxide at 37^{o}C. For uptake assays, 0.5 million HEK293 cells/well were plated in 24-well plate for 24 h. For uptake assays using PHH, cryopreserved hepatocytes were thawed and plated 0.35 million per well in 24-well collagen-coated plate with 0.5 ml/well TORPEDO containing INVITROGRO CP medium (1:9 v/v) for 5 h.

To determine [^{14}C]-metformin uptake, HEK293 cells or PHH were washed three times with HK buffer (4.8 mM KCl, 1.2 mM K_2HPO_4, 1.2 mM $MgSO_4$, 5.6 mM glucose, 25 mM HEPES, 12 mM $CaCl_2$, 125 mM NaCl, 25 mM $NaHCO_3$) and incubated at 37^{O}C. To initiate uptake, 500µl of HK buffer containing 5 µM or 20 µM [^{14}C]-metformin (for HEK293 cells or PHH, respectively) with or without inhibitor (pre-incubated at 37^{O}C) were added to the cells. After an appropriate time (over a period where uptake was linear; 5 min for HEK293 cells and 15 min for PHH), [^{14}C]-metformin uptake into the cells was terminated by removing [^{14}C]-metformin containing solution and immediately washing it 3 times with ice-cold HK buffer. Then, cells were lysed by adding 1 ml of 2% SDS solution to each well and incubating them on a shaker at 125 rpm for 1 h at 37^{O}C. After 1 h, 700 µL of lysed solution from each well was used to measure radioactivity by Tri-Carb Liquid Scintillation Counters (PerkinElmer, Waltham (MA)). In addition, 50 µL of lysed solution was used to

DMD Fast Forward. Published on August 25, 2020 as DOI: 10.1124/dmd.120.000156
This article has not been copyedited and formatted. The final version may differ from this version.

measure protein content using the BCA method. [^{14}C]-metformin uptake CL into the cells was calculated by the ratio of rate of [^{14}C]-metformin uptake and the [^{14}C]-metformin concentration in the media. Uptake $CL_{int,\textit{in vitro}}$ was calculated by dividing slope of [^{14}C]-metformin accumulation over time by [^{14}C]-metformin concentration in media. CL_{int} calculated in absence and presence of inhibitor was considered as total CL ($CL_{int,\ total}$) and passive CL ($CL_{int,\textit{in vitro},\ passive}$), respectively. Active CL ($CL_{int,\textit{in vitro},\ active}$) was calculated by subtracting $CL_{int,\textit{in vitro},passive}$ from $CL_{int,\textit{in vitro},total}$.

To determine the contribution of OCT1 or thiamine transporter 2 (THTR2) to [^{14}C]-metformin transport into PHH, [^{14}C]-metformin uptake assays were conducted in the presence or absence of 500 µM quinidine or 400mM thiamine (a THTR2 substrate with Km of 3.4 mM (Liang et al., 2015)), respectively.

Quantification of total and percent plasma membrane abundance (PMA) of OCT1 in HEK293 cells

Data for the total and PMA of OCT1 in PHH were obtained from our previous publication (Kumar et al., 2019). OCT1 total and PMA in HEK293 cells was quantified using our previous published biotinylation approach (Kumar et al., 2017). HEK293 cells were grown in three independent experiment in 75 cm^2 flask until 80% confluency and incubated at 37^{o}C with 10 ml of 0.78 mg/ml sulfo-NHS-SS-biotin. After 1 h, cells were lysed and 50 µl of cell lysate was separated to quantify total abundance. From rest of the total cell lysate, the biotinylated plasma membrane fragments (to quantify %PMA) were separated from the total cell lysate and intracellular membranes using the neutravidin resin columns. Briefly,

DMD Fast Forward. Published on August 25, 2020 as DOI: 10.1124/dmd.120.000156
This article has not been copyedited and formatted. The final version may differ from this version.

0.2 mg of total protein homogenate and biotinylated fraction were denatured adding 45 µl of 100 mM ammonium bicarbonate buffer pH 7.8, 25 µl of 3% sodium deoxycholate (w/v), 12.5 µl of 250 mM DTT and 5 µl of 10 mg/ml human albumin and incubated at 95^{O}C for 5 mins. After incubation, samples were returned to room temperature and 25 µl of 200 mM IAA were added and samples were incubated in the dark for 30 mins. Then, 500 µl of ice-cold methanol, 200 µl of chloroform and 450 µl of water were added. Samples were mixed and centrifuged at 12,000 g for 10 mins. Precipitated protein samples were re-dissolved in in 45 µl of 100 mM ammonium bicarbonate buffer and digested with 20 µl (~3.2 µg) of trypsin for 18 h at 37^{O}C in a shaker (300rpm). Finally, the digestion was terminated by adding to the sample 20 µl of ice-cold acetonitrile containing the internal standard. Then, the sample was centrifuged at 5,000 g for 5 min at 4^{O}C. The supernatant was collected and analyzed on AB Sciex 6500 triple-quadrupole mass spectrometer (Sciex, Framingham, MA) coupled to the Water Acquity UPLC system (Waters Corporation, Milford, MA) operated in electrospray positive ionization mode using previously described approach (Prasad et al., 2016). An acquity UPLC HSS T3 Column, (1.8 mm, 2.1 100 mm) with a 0.2 mm inlet frits (Waters) was used for chromatographic separation and resolution. The flow rate of mobile phase was 0.3 ml/min using gradient ranging from 3-90 % acetonitrile/ water containing 0.1% formic acid. Signature peptides and product ions as well as their respective SIL peptides used to quantify proteins were obtained from our previous report (Kumar et al., 2019). The ratio of abundance of protein in biotinylated fractions and total lysate was used to determine percent plasma membrane abundance (%PMA).

DMD Fast Forward. Published on August 25, 2020 as DOI: 10.1124/dmd.120.000156
This article has not been copyedited and formatted. The final version may differ from this version.

Estimation of *in vivo* [$_{11}$C]-metformin $CL_{h,s,in}$ by compartmental modeling of PET imaging data

PET-imaged metformin hepatic radioactivity concentrations-time data previously published by Gormsen et al. (Gormsen et al., 2016) were reanalyzed using a blood input function and a one-tissue compartment model **(Fig 3A)** with a fixed blood volume (SAAMII). This differed from the published analysis where radioactivity from the volume of blood within the liver tissue was not taken into account, plasma concentrations were used as input and a two-compartment model was used (Gormsen et al., 2016).

$$\frac{dA_L}{dt} = CL_{h,s,in} \cdot C_B - CL_{h,s,ef} \cdot C_L \quad \text{(Equation 1)}$$

$$C_B = C_{Venous} \cdot 0.8 + C_{Arterial} \cdot 0.2 \quad \text{(Equation 2)}$$

Where A, C, B, L, $CL_{h,s,in}$ and $CL_{h,s,ef}$ represents amount, concentration, blood, liver, sinusoidal uptake CL, sinusoidal efflux CL, biliary efflux CL and metabolic CL respectively. Since, no biliary efflux was observed and majority of metformin is excreted renally unchanged, biliary clearance and metabolic clearance were not included in equation 1 (Hardie, 2007; Graham et al., 2011; Gormsen et al., 2016). The hepatic input blood concentration is a sum of the input via the portal vein (80%) and the hepatic artery (20%) (Schenk et al., 1962) where $C_{Arterial}$ and C_{Venous} are the observed [^{11}C]-metformin arterial and portal vein concentrations respectively (Eq. 2). The volume of the liver was determined based on Eq. 3 (Chan et al., 2006).

DMD Fast Forward. Published on August 25, 2020 as DOI: 10.1124/dmd.120.000156
This article has not been copyedited and formatted. The final version may differ from this version.

Liver weight (g) = 218.32 + body weight (kg) x 12.29 + gender x 50.74

(Equation 3)

For male and female, gender = 1 and 0, respectively. The volume of blood in the liver were fixed to 10% of total blood volume estimated based on body weight (75 mL/kg for males and 65 mL/kg for females) (Lautt, 1977; Stabin and Siegel, 2003; Pham and Shaz, 2013). Goodness of fit of the model to the data was assessed by the weighted residual plots, visual inspection of the predicted and observed data and the confidence (CV%) in the estimates of the parameters.

Prediction of the *in vivo* metformin blood hepatic uptake CL from PHH using the MGPGL approach

Metformin *in vivo* blood intrinsic hepatic sinusoidal uptake CL ($\mathrm{CL_{int,s,in}}$) was predicted from PHH data using the MGPGL approach (Eq. 4).

$$\mathrm{CL_{int,s,in}} = \frac{\mathrm{CL_{int,PHH,total}} \times \text{Liver weight} \times \text{MGPGL}}{\text{B:P}} \quad \text{(Equation 4)}$$

Liver weight was assumed to be 1500 g, B:P is the blood to plasma ratio (0.6) and MGPGL was 120 mg of total protein per gram of liver based on a previous report (1.2 X10^8 cells/g liver and 1 million cells ~1mg protein) (Jones et al., 2012; Gormsen et al., 2016; Kim et al., 2019).

Then, metformin sinusoidal uptake clearance was computed using the well-stirred model (WSHM).

DMD Fast Forward. Published on August 25, 2020 as DOI: 10.1124/dmd.120.000156
This article has not been copyedited and formatted. The final version may differ from this version.

$$\mathrm{CL_{h,s,in}} = \frac{\mathrm{Q} * \mathrm{fu} * \mathrm{CL_{int,s,in}}}{\mathrm{Q} + \mathrm{fu} * \mathrm{CL_{int,s,in}}} \qquad \text{(Equation 5)}$$

Where, fu is the fraction of metformin unbound in plasma (assumed to be 1) and Q is the hepatic blood flow (1,500 ml/min) (Scheen, 1996).

Prediction of *in vivo* metformin hepatic uptake CL from OCT1- HEK293 cells and PHH using the REF approach

In vivo blood metformin hepatic intrinsic sinusoidal active uptake CL ($CL_{int,s,active\ in}$) was determined from *in vitro* metformin uptake CL in OCT1-HEK293 cells or PHH using the REF approach, corrected for OCT1 PMA in these cells or PHH ($\%\mathrm{PMA}_{in-vitro}$; Eq. 6). In doing so, the following assumptions were made: 1) OCT1 is the only transporter responsible for metformin hepatic uptake (see results for justification), and 2) because it is impossible to use the biotinylation method for quantification of OCT1 PMA in liver tissue, the PMA abundance of OCT1 in liver tissue ($\%\mathrm{PMA_{ex\ vivo}}$) was assumed to be 100%.

$$\mathrm{CL_{int,s,active\ in}} = \frac{\mathrm{CL}_{int,in\ vitro,\mathrm{active}} \times \frac{[\mathrm{E}]_{ex\ vivo}}{[\mathrm{E}]_{in\ vitro}} \times \frac{\%\mathrm{PMA}_{ex\ vivo}}{\%\mathrm{PMA}_{in\ vitro}} \times \mathrm{MGMPGL} \times \mathrm{Liver\ weight}}{\mathrm{B{:}\,P}}$$

(Equation 6)

$[\mathrm{E}]_{in\ vitro}$ is OCT1 abundance in HEK293 cells or PHH. $[\mathrm{E}]_{ex\ vivo}$ is total OCT1 abundance in human liver tissue and MGMPGL is mg protein of total membrane protein

DMD Fast Forward. Published on August 25, 2020 as DOI: 10.1124/dmd.120.000156
This article has not been copyedited and formatted. The final version may differ from this version.

per gram of liver from individual control liver (n=36) obtained from our previous report (Wang et al., 2016).

Also, the blood hepatic intrinsic sinusoidal passive uptake CL of metformin ($\mathrm{CL}_{\mathrm{int,s,passive\ in}}$) was scaled based on liver weight was adjusted for the sinusoidal surface area (SSA) (37%; Eq. 7) since the entire plasma membrane of hepatocytes is not exposed to blood (Esteller, 2008). The correction for SSA was not made for the active uptake of metformin into cells since OCT1 is thought to be present only on the sinusoidal membrane of the hepatocytes.

$$\mathrm{CL}_{\mathrm{int,s,passive,in}} = \frac{\mathrm{CL}_{\mathrm{int},in\ vitro,\mathrm{passive}} \times \mathrm{MGPGL} \times \%\ \mathrm{SSA} \times \mathrm{Liver\ weight}}{\mathrm{B{:}P}} \qquad \text{(Equation 7)}$$

Finally, the total blood intrinsic hepatic sinusoidal uptake CL($\mathrm{CL}_{\mathrm{int,s,in}}$) was computed (Eq. 8) to estimate the sinusoidal hepatic uptake clearance ($\mathrm{CL}_{\mathrm{h,s,in}}$) using the WSHM (Eq. 5).

$$\mathrm{CL}_{\mathrm{int,s,in}} = \mathrm{CL}_{\mathrm{h,s,active\ in}} + \mathrm{CL}_{\mathrm{h,s,passive\ in}} \qquad \text{(Equation 8)}$$

Data are presented as the mean of REF-predicted $\mathrm{CL}_{\mathrm{h,s,in}}$ based on 36 control livers while the mean MGPGL-predicted $\mathrm{CL}_{\mathrm{h,s,in}}$ was computed as a mean of four different lots of PHH.

Results

DMD Fast Forward. Published on August 25, 2020 as DOI: 10.1124/dmd.120.000156
This article has not been copyedited and formatted. The final version may differ from this version.

[^{14}C]-metformin uptake into hepatocytes is mediated by OCT1 and not THTR2

Since [^{14}C]-metformin uptake was linear in PHH over period of 15 mins **(Fig 2)**, this was the time used to determine [^{14}C]-metformin uptake into PHH in the presence and absence of OCT (quinidine) or THTR2 (thiamine) inhibitor **(Fig 1)**. Quinidine, but not thiamine, significantly inhibited metformin uptake by 83%, 68.1% and 63.5% in ADR, JEL and YTW PHH, respectively.

Estimation of [^{14}C]-metformin CLint uptake into HEK293 cells or PHH.

[^{14}C]-metformin uptake into HEK293 cells and PHH was linear over 5 min and 15 min respectively **(Fig 2A-E)**. The mean [^{14}C]-metformin $\mathrm{CL}_{int,\mathrm{PHH,passive}}$ or $\mathrm{CL}_{int,\mathrm{OCT1-HEK293,passive}}$ was similar to $\mathrm{CL}_{int,\mathrm{mock-HEK293,total}}$ or $\mathrm{CL}_{int,\mathrm{mock-HEK293,passive}}$. These data further confirm that [^{14}C]-metformin uptake into hepatocytes is mediated primarily by OCT1 **(Table 1)**.

Plasma and total membrane abundance (PMA) of OCT1 in OCT1-HEK293 cells and PHH

The percent PMA of OCT1, Na^+ K^+ATPase (plasma membrane marker) and calreticulin (endoplasmic reticulum marker) in HEK293 cells was 36.04±2.46%, 58.73±2.79% and 6.63±0.39%, respectively. The low presence of calreticuin in the plasma membrane

DMD Fast Forward. Published on August 25, 2020 as DOI: 10.1124/dmd.120.000156
This article has not been copyedited and formatted. The final version may differ from this version.

fraction demonstrated the fidelity of the bitoinylation method. The percent PMA of OCT1 in PHH used in this study (ADR: 63.8%, FEA: 55.3%, JEL: 51.9%, YTW: 65.8%) was obtained from our previous report (Kumar et al., 2019). These PMA data, together with the total abundance of OCT1 in these cells, were used (Eq. 5) to predict the *in vivo* metformin hepatic uptake clearance (see below and Table 4).

Estimating *in vivo* [^{11}C]-metformin hepatic uptake CL from PET imaging data after correcting for blood [^{11}C]-metformin content in the liver

The mean estimate of [^{11}C]-metformin $CL_{h,s,in}$ in 4 subjects was 441±76 ml/min (range 361-552 ml/min) with each subject's $CL_{h,s,in}$ estimated with a high degree of confidence (low %CV of the estimates) **(Table 2).**

***In vitro* to *in vivo* extrapolation (IVIVE) of metformin hepatic sinusoidal uptake CL from HEK293 cells and PHH using REF vs. the MGPGL approach**

IVIVE of metformin $CL_{h,s,in}$ based on the MGPGL approach significantly underpredicted (by more than 56%) the observed value **(Fig 4A, Table 3)**. Likewise, IVIVE of metformin $CL_{h,s,in}$ based on total abundance of OCT1 (i.e. without correcting for PMA) in HEK293 cells or PHH under-predicted the observed value **(Fig 4B, Table 4)**. In addition, except for PHH JEL and YTW, the predicted $CL_{h,s,in}$ based on HEK293 cells or PHH (average or ADR or FEA) were below the predefined acceptance criteria for prediction of the observed *in vivo* $CL_{h,s,in.}$ In contrast, after correcting for PMA, the predicted $CL_{h,s,in}$ based on HEK293 cells or the average PHH were within predefined acceptance criteria with the latter under-predicting the observed value much more than the former.

DMD Fast Forward. Published on August 25, 2020 as DOI: 10.1124/dmd.120.000156
This article has not been copyedited and formatted. The final version may differ from this version.

Discussion

The major findings of this study are: 1) metformin is transported into human hepatocytes predominantly by OCT1 with no (or little) contribution from THTR2; 2) PET imaging data should be corrected for hepatic blood metformin content to correctly estimate the *in vivo* metformin $CL_{h,s,in}$; 3) the REF approach is superior to the MGPGL approach in accurately predicting the *in vivo* $CL_{h,s,in}$ of metformin.

In humans, hepatic uptake of metformin (the site of its pharmacological effect) is purely a distributional CL because metformin is not metabolized or biliary excreted by the liver and is primarily (99%) eliminated unchanged in the urine (Pentikainen et al., 1979). The latter was confirmed in the human PET imaging study where no metformin radioactivity could be detected in the gallbladder (Gormsen et al., 2016). Various *in vitro* studies have confirmed that metformin is transported into the liver primarily by OCT1 (Km 1.2mM) (Kimura et al., 2005). Although OCT3 can transport metformin (Km 1.1 mM) (Chen et al., 2010), because the hepatic protein abundance of OCT3, relative to OCT1, is negligible (Drozdzik et al., 2018), we assumed that it did not contribute to the total uptake of metformin either *in vivo* or in vitro. THTR2, a thiamine transporter, has also been found to transport metformin (Km 1.15 mM) (Liang et al., 2015). Therefore, we determined its contribution in the transport of metformin into PHH using sufficiently high concentration (400 mM) of thiamine to completely inhibit THTR2. We found that THTR2 does not significantly contribute towards metformin transport into PHH **(Fig 1)**. This was confirmed

DMD Fast Forward. Published on August 25, 2020 as DOI: 10.1124/dmd.120.000156
This article has not been copyedited and formatted. The final version may differ from this version.

by our findings that metformin uptake CL into PHH was similar to that in OCT1-HEK293 cells when OCT1 was completely inhibited by quinidine in both systems **(Fig 2, Table 1)**.

Prior to predicting metformin $CL_{h,s,in}$ by scaling $CL_{int,in\ vitro}$ in OCT1-HEK293 cells or PHH, we estimated the *in vivo* metformin $CL_{h,s,in}$ by reanalysis of previously published PET imaging data. Reanalysis was performed because estimates of hepatic uptake CL (whether *in vivo* or *in vitro* into hepatocytes) of a drug is primarily derived from data in the initial uptake phase. In the case of PET imaging, because the liver has a significant amount of blood (10% of total blood volume) and the radioactivity content in hepatic tissue during the initial uptake phase may not be significantly larger than that in the blood, the drug content in the blood in the liver will upwardly bias the true hepatic uptake CL of the drug. Indeed, this was the case for metformin, the previously reported [^{11}C]-metformin plasma $CL_{h,s,in}$ was 0.55±0.15 ml/min/ml (or 0.55±0.15 ml/min/g; assuming density of liver tissue as 1.0) of hepatic tissue (or blood $CL_{h,s,in}$ 1375±375 ml/min assuming 1.5 Kg as liver weight by PET imaging (Gormsen et al., 2016). On reanalysis of these PET imaging data, where we took into consideration the significance presence of blood in the liver, the estimated $CL_{h,s,in}$ was found to be 441 ml/min, i.e. ~32% of the previously reported values **(Table 2)**.

When we used the REF approach to predict $CL_{h,s,in}$ based on the assumption that 100% of OCT1 was present on the plasma membrane of both HEK293 cells or PHH (average abundance), the $CL_{h,s,in}$ was under-predicted by ~ 60% for both *in vitro* systems **(Fig 4**

DMD Fast Forward. Published on August 25, 2020 as DOI: 10.1124/dmd.120.000156
This article has not been copyedited and formatted. The final version may differ from this version.

and Table 4). The predicted $CL_{h,s,in}$ by the individual lots of hepatocytes was also under-predicted but that by the JEL and YTW was within 2-fold of the acceptance criteria. Since only OCT1 present in the plasma membrane is functional, and not all the OCT1 transporters are present in the plasma membrane of HEK293 cells or PHH, we asked if correcting for PMA of OCT1 improved our prediction of $CL_{h,s,in}$. This question was also motivated by our previous finding that such a correction allowed for better prediction of *in vivo* metformin secretory renal CL in humans (Kumar et al., 2018). Indeed, after correcting for PMA, OCT1- HEK293 cells predicted a value for $CL_{h,s,in}$ (405±122 ml/min) that was not significantly different from that observed from PET imaging (441±76 ml/min). Likewise, after correcting for PMA, data from the PHH, on average, predicted a value for $CL_{h,s,in}$ (230±78 ml/min) that was within the lower limit of 2-fold predefined acceptance criteria (221 ml/min). In addition, except for ADR and FEA, the remaining lots of PHH predicted metformin $CL_{h,s,in}$ within the predefined acceptance criteria. In contrast, the traditional MGPGL approach (on average) underpredicted $CL_{uptake,h}$ by more than 56% (ranging from 47-64%) **(Table 3 and Fig 4A)**. This observation is consistent with previous reports that PHH underpredict the hepatic uptake CL of several drugs (Jones et al., 2012). One possible reason proposed for such underprediction is the protein-mediated effect on hepatic uptake CL (Miyauchi et al., 2018; Bteich et al., 2019). However, this is unlikely to explain our findings since metformin is not bound to plasma proteins. Another potential explanation is that the value of MGPGL used is incorrect. Taken together these results clearly demonstrate that PMA-corrected REF approach is superior to the traditional MGPGL approach when predicting $CL_{h,s,in}$ of metformin. We have also demonstrated that REF approach is superior to the MGPGL approach when predicting $CL_{h,s,in}$ of

DMD Fast Forward. Published on August 25, 2020 as DOI: 10.1124/dmd.120.000156
This article has not been copyedited and formatted. The final version may differ from this version.

rosuvastatin (an OATP substrate) in the rat (Ishida et al., 2018). Thus, the REF approach appears to be superior to the MGPGL approach for a diverse set of drugs which are transported by different transporters. Additional studies need to be conducted to determine if this conclusion can be generalized across a larger number of drugs transported by a variety of transporters.

ACKNOWLEDGMENTS

The authors thank Tot Bui Nguyen for her support in cell-surface biotinylation experiments and LC-MS/MS proteomics.

AUTHORSHIP CONTRIBUTIONS

Participated in research design: Sachar, Kumar, and Unadkat. Conducted experiments: Sachar. Performed data analysis: Sachar. Wrote or contributed to the manuscript: Sachar, Munk, Gormsen and Unadkat.

REFERENCES

Andersson TB, Sjoberg H, Hoffmann KJ, Boobis AR, Watts P, Edwards RJ, Lake BG, Price RJ, Renwick AB, Gomez-Lechon MJ, Castell JV, Ingelman-Sundberg M, Hidestrand M, Goldfarb PS, Lewis DF, Corcos L, Guillouzo A, Taavitsainen P, and Pelkonen O (2001) An assessment of human liver-derived in vitro systems to predict the in vivo metabolism and clearance of almokalant. *Drug Metab Dispos* **29:**712-720.

Bosgra S, van de Steeg E, Vlaming ML, Verhoeckx KC, Huisman MT, Verwei M, and Wortelboer HM (2014) Predicting carrier-mediated hepatic disposition of rosuvastatin in man by scaling from individual transfected cell-lines in vitro using absolute transporter protein quantification and PBPK modeling. *Eur J Pharm Sci* **65:**156-166.

Bteich M, Poulin P, and Haddad S (2019) The potential protein-mediated hepatic uptake: discussion on the molecular interactions between albumin and the hepatocyte cell surface and their implications for the in vitro-to-in vivo extrapolations of hepatic clearance of drugs. *Expert Opin Drug Metab Toxicol* **15:**633-658.

Chan SC, Liu CL, Lo CM, Lam BK, Lee EW, Wong Y, and Fan ST (2006) Estimating liver weight of adults by body weight and gender. *World J Gastroenterol* **12:**2217-2222.

Chen L, Pawlikowski B, Schlessinger A, More SS, Stryke D, Johns SJ, Portman MA, Chen E, Ferrin TE, Sali A, and Giacomini KM (2010) Role of organic cation transporter 3 (SLC22A3) and its missense variants in the pharmacologic action of metformin. *Pharmacogenet Genomics* **20:**687-699.

Drozdzik M, Busch D, Lapczuk J, Muller J, Ostrowski M, Kurzawski M, and Oswald S (2018) Protein Abundance of Clinically Relevant Drug Transporters in the Human Liver and Intestine: A Comparative Analysis in Paired Tissue Specimens. *Clin Pharmacol Ther*.

Esteller A (2008) Physiology of bile secretion. *World J Gastroenterol* **14:**5641-5649.

Gormsen LC, Sundelin EI, Jensen JB, Vendelbo MH, Jakobsen S, Munk OL, Hougaard Christensen MM, Brosen K, Frokiaer J, and Jessen N (2016) In Vivo Imaging of Human 11C-Metformin in Peripheral Organs: Dosimetry, Biodistribution, and Kinetic Analyses. *J Nucl Med* **57:**1920-1926.

Graham GG, Punt J, Arora M, Day RO, Doogue MP, Duong JK, Furlong TJ, Greenfield JR, Greenup LC, Kirkpatrick CM, Ray JE, Timmins P, and Williams KM (2011) Clinical pharmacokinetics of metformin. *Clin Pharmacokinet* **50:**81-98.

Hardie DG (2007) AMP-activated protein kinase as a drug target. *Annu Rev Pharmacol Toxicol* **47:**185-210.

Ishida K, Ullah M, Toth B, Juhasz V, and Unadkat JD (2018) Successful Prediction of In Vivo Hepatobiliary Clearances and Hepatic Concentrations of Rosuvastatin Using Sandwich-Cultured Rat Hepatocytes, Transporter-Expressing Cell Lines, and Quantitative Proteomics. *Drug Metab Dispos* **46:**66-74.

Jones HM, Barton HA, Lai Y, Bi YA, Kimoto E, Kempshall S, Tate SC, El-Kattan A, Houston JB, Galetin A, and Fenner KS (2012) Mechanistic pharmacokinetic modeling for the prediction of transporter-mediated disposition in humans from sandwich culture human hepatocyte data. *Drug Metab Dispos* **40:**1007-1017.

Kim SJ, Lee KR, Miyauchi S, and Sugiyama Y (2019) Extrapolation of In Vivo Hepatic Clearance from In Vitro Uptake Clearance by Suspended Human Hepatocytes for Anionic Drugs with High Binding to Human Albumin: Improvement of In Vitro-to-In Vivo Extrapolation by Considering the "Albumin-Mediated" Hepatic Uptake Mechanism on the Basis of the "Facilitated-Dissociation Model". *Drug Metab Dispos* **47:**94-103.

Kimura N, Masuda S, Tanihara Y, Ueo H, Okuda M, Katsura T, and Inui K (2005) Metformin is a superior substrate for renal organic cation transporter OCT2 rather than hepatic OCT1. *Drug Metab Pharmacokinet* **20:**379-386.

Kumar V, Nguyen TB, Toth B, Juhasz V, and Unadkat JD (2017) Optimization and Application of a Biotinylation Method for Quantification of Plasma Membrane Expression of Transporters in Cells. *AAPS J* **19:**1377-1386.

Kumar V, Salphati L, Hop C, Xiao G, Lai Y, Mathias A, Chu X, Humphreys WG, Liao M, Heyward S, and Unadkat JD (2019) A Comparison of Total and Plasma Membrane Abundance of Transporters in Suspended, Plated, Sandwich-Cultured Human Hepatocytes vs. Human Liver Tissue Using Quantitative Targeted Proteomics and Cell-Surface Biotinylation. *Drug Metab Dispos*.

Kumar V, Yin J, Billington S, Prasad B, Brown CDA, Wang J, and Unadkat JD (2018) The Importance of Incorporating OCT2 Plasma Membrane Expression and Membrane Potential in IVIVE of Metformin Renal Secretory Clearance. *Drug Metab Dispos* **46:**1441-1445.

Lautt WW (1977) Hepatic vasculature: a conceptual review. *Gastroenterology* **73:**1163-1169.

Liang X, Chien HC, Yee SW, Giacomini MM, Chen EC, Piao M, Hao J, Twelves J, Lepist EI, Ray AS, and Giacomini KM (2015) Metformin Is a Substrate and Inhibitor of the Human Thiamine Transporter, THTR-2 (SLC19A3). *Mol Pharm* **12:**4301-4310.

Miyauchi S, Masuda M, Kim SJ, Tanaka Y, Lee KR, Iwakado S, Nemoto M, Sasaki S, Shimono K, Tanaka Y, and Sugiyama Y (2018) The Phenomenon of Albumin-Mediated Hepatic Uptake of Organic Anion Transport Polypeptide Substrates: Prediction of the In Vivo Uptake Clearance from the In Vitro Uptake by Isolated Hepatocytes Using a Facilitated-Dissociation Model. *Drug Metab Dispos* **46:**259-267.

Obach RS, Baxter JG, Liston TE, Silber BM, Jones BC, MacIntyre F, Rance DJ, and Wastall P (1997) The prediction of human pharmacokinetic parameters from preclinical and in vitro metabolism data. *J Pharmacol Exp Ther* **283:**46-58.

Pakkir Maideen NM, Jumale A, and Balasubramaniam R (2017) Drug Interactions of Metformin Involving Drug Transporter Proteins. *Adv Pharm Bull* **7:**501-505.

Pentikainen PJ, Neuvonen PJ, and Penttila A (1979) Pharmacokinetics of metformin after intravenous and oral administration to man. *Eur J Clin Pharmacol* **16:**195-202.

Pham HP and Shaz BH (2013) Update on massive transfusion. *BJA: British Journal of Anaesthesia* **111:**i71-i82.

Prasad B, Johnson K, Billington S, Lee C, Chung GW, Brown CD, Kelly EJ, Himmelfarb J, and Unadkat JD (2016) Abundance of Drug Transporters in the Human Kidney Cortex as Quantified by Quantitative Targeted Proteomics. *Drug Metab Dispos* **44:**1920-1924.

Rostami-Hodjegan A and Tucker GT (2007) Simulation and prediction of in vivo drug metabolism in human populations from in vitro data. *Nat Rev Drug Discov* **6:**140-148.

Rowland M, Peck C, and Tucker G (2011) Physiologically-based pharmacokinetics in drug development and regulatory science. *Annu Rev Pharmacol Toxicol* **51:**45-73.

Scheen AJ (1996) Clinical pharmacokinetics of metformin. *Clin Pharmacokinet* **30:**359-371.

Schenk WG, Jr., Mc DJ, Mc DK, and Drapanas T (1962) Direct measurement of hepatic blood flow in surgical patients: with related observations on hepatic flow dynamics in experimental animals. *Ann Surg* **156:**463-471.

Soars MG, McGinnity DF, Grime K, and Riley RJ (2007) The pivotal role of hepatocytes in drug discovery. *Chem Biol Interact* **168:**2-15.

Stabin MG and Siegel JA (2003) Physical models and dose factors for use in internal dose assessment. *Health Phys* **85:**294-310.

Vildhede A, Mateus A, Khan EK, Lai Y, Karlgren M, Artursson P, and Kjellsson MC (2016) Mechanistic Modeling of Pitavastatin Disposition in Sandwich-Cultured Human Hepatocytes: A Proteomics-Informed Bottom-Up Approach. *Drug Metab Dispos* **44:**505-516.

Wang L, Collins C, Kelly EJ, Chu X, Ray AS, Salphati L, Xiao G, Lee C, Lai Y, Liao M, Mathias A, Evers R, Humphreys W, Hop CE, Kumer SC, and Unadkat JD (2016) Transporter Expression in Liver Tissue from Subjects with Alcoholic or Hepatitis C Cirrhosis Quantified by Targeted Quantitative Proteomics. *Drug Metab Dispos* **44:**1752-1758.

DMD Fast Forward. Published on August 25, 2020 as DOI: 10.1124/dmd.120.000156
This article has not been copyedited and formatted. The final version may differ from this version.

Footnotes

Research was supported by University of Washington Research Affiliate Program on Transporters (UWRAPT) funded by Genentech, Biogen, Gilead, Merck and Takeda

DMD Fast Forward. Published on August 25, 2020 as DOI: 10.1124/dmd.120.000156
This article has not been copyedited and formatted. The final version may differ from this version.

Figure Legend

Figure 1. [^{14}C]-metformin uptake into three lots of PHH in the absence and presence of an OCT1 or a THTR2 inhibitor. Quinidine (500μM), an OCT inhibitor, significantly inhibited hepatocyte uptake of metformin whereas thiamine (400mM), a THTR2 inhibitor, did not. Data are presented as mean ± S.D. of triplicate determinations. Data were analyzed by one-way analysis of variance followed by Tukey multiple comparison post hoc test. *, $P < 0.05$ compared with the respective control.

Figure 2. Estimation of [^{14}C]-metformin uptake CL_{int} into HEK 293 cells or PHH. [^{14}C]-metformin uptake into OCT1-expressing HEK 293 and mock cells (A) or into four different lots of PHH (B-E) was linear over a period of 5 mins and 15 mins, respectively. Data in A-E are presented as mean ± S.D. of experiments conducted in triplicate.

Figure 3. Estimate of the in vivo [^{11}C]-metformin hepatic uptake clearance after correcting for blood [^{11}C]-metformin content in the liver. [^{11}C]-metformin hepatic concentrations calculated from PET imaging and corresponding plasma [^{11}C]-metformin concentrations were obtained from a previous publication (Gormsen et al., 2016). A one compartment pharmacokinetic model (A), which incorporated correction for blood [^{11}C]-metformin content in the liver, was fitted to the hepatic [^{11}C]-metformin concentration versus time data in 5 subjects. Arterial plus image estimated portal venous blood [^{11}C]-metformin concentrations were used as the input function using the forcing function (FF) approach. Observed (diamonds) and model fitted hepatic [^{11}C]-

DMD Fast Forward. Published on August 25, 2020 as DOI: 10.1124/dmd.120.000156
This article has not been copyedited and formatted. The final version may differ from this version.

metformin concentration vs. time profile in a representative subject demonstrates relatively good fit of the model to the data (B).

Figure 4. *In vitro* to *in vivo* extrapolation of metformin hepatic sinusoidal uptake clearance $(\mathrm{CL}_{\mathrm{h,s,in}})$ **based on HEK293 cells or PHH.** For all four lots of PHH, the predicted $\mathrm{CL}_{\mathrm{h,s,in}}$ based on the MGPGL approach, under-predicted the observed value (continuous line) and also fell outside the 2-fold predefined acceptance criteria (dashed line. A). Likewise, the predicted metformin $\mathrm{CL}_{\mathrm{h,s,in}}$ based on total abundance of OCT1 (i.e. without correcting for PMA) in HEK293 cells or PHH under-predicted the observed value (B). In contrast, after correcting for PMA, the predicted metformin $\mathrm{CL}_{\mathrm{h,s,in}}$ based on HEK293 cells or the average PHH were within the predefined acceptance criteria with the latter under-predicting the observed value more than the former. Data shown are mean ±S.D.

DMD Fast Forward. Published on August 25, 2020 as DOI: 10.1124/dmd.120.000156
This article has not been copyedited and formatted. The final version may differ from this version.

Table 1. Total and passive [^{14}C]-metformin (500μM) uptake clearances ($CL_{int,in\ vitro}$) into PHH and HEK293 cells estimated in the absence and presence of quinidine respectively

Cell	$CL_{int,in\ vitro}$ (μl/min/mg protein)*	
	-Quinidine	+Quinidine
HEK293: OCT1	8.27±5.8	0.22±0.06
HEK293: Mock	0.17±0.10	0.29± 0.007
PHH: ADR	0.88	0.07
PHH: FEA	0.64	0.04
PHH: JEL	0.79	0.15
PHH: YTW	0.55	0.10

* from either three (HEK293 cells; mean ± S.D) or two independent experiments (PHH; mean)

DMD Fast Forward. Published on August 25, 2020 as DOI: 10.1124/dmd.120.000156
This article has not been copyedited and formatted. The final version may differ from this version.

Table 2. Estimate of [^{11}C]- metformin hepatic uptake clearance from the PET imaging study

Subject	$CL_{h,s,in}$ (ml/min)		
	Value	**% CV***	**95% CI***
1	388	34	127-650
2	361	26	155-568
3	552	30	226-878
4	427	38	102-751
5	476	25	236-715
Mean ±SD	441±76		

* %CV (coefficient of variation) and 95% CI (confidence interval) represent the confidence in the $CL_{h,s,in}$ (ml/min) estimate

DMD Fast Forward. Published on August 25, 2020 as DOI: 10.1124/dmd.120.000156
This article has not been copyedited and formatted. The final version may differ from this version.

Table 3. IVIVE of metformin $CL_{h,s,in}$ based on the traditional MGPGL approach

	PHH				
	ADR	**FEA**	**JEL**	**YTW**	**Average ±SD**
$CL_{int,PHH,total}$ (µl/min/mg protein)	0.88±0.12	0.64±0.07	0.79±0.10	0.55±0.02	0.72±0.15
Protein yield MGPGL(mg protein/g of liver)			120[a]		
Assumed liver weight (g)			1500		
Predicted $CL_{h,s,in}$ (ml/min) (Eq. 4)	264±37	193±22	240±32	167±7	216±44
$CL_{h,s,in}$ (ml/min) based on the WSHM (Eq. 5)	225±28	171±17	206±24	150±5	188±34

a. Value for the yield of total mg protein per gram of liver was obtained based on hypocellularity and total protein per million hepatocytes (Jones et al., 2012; Kim et al., 2019)

DMD Fast Forward. Published on August 25, 2020 as DOI: 10.1124/dmd.120.000156
This article has not been copyedited and formatted. The final version may differ from this version.

Table 4. IVIVE of metformin $CL_{h,s,in}$ based on the REF-approach

	HEK293	PHH				
		ADR	FEA	JEL	YTW	Average ±SD
$CL_{int,in\ vitro,active}$ (µl/min/mg protein)	8.05±0.64	0.81±0.06	0.60 ±0.05	0.65 ±0.45	0.45 ±0.08	0.63±0.15
$CL_{int,in\ vitro,\mathrm{passive}}$ (µl/min/mg protein)	0.22 ±0.06	0.07±0.06	0.04±0.02	0.15±0.07	0.1±0.06	0.09±0.05
in vitro total OCT1 protein abundance (pmol/mg protein)	17.34±0.35	3.21±0.12[a]	1.92±0.33[a]	1.04±0.06[a]	0.71±0.04[a]	1.72±1.12
ex vivo hepatic tissue OCT1 protein abundance (pmol/mg protein)[b]			4.68±1.9			
Scaling factor (SF) : $[E]_{ex\ vivo}/[E]_{in\ vitro}$	0.27	1.46	2.43	4.5	6.59	3.75±2.28
Protein yield MGMPGL (mg total membrane protein/g of liver)[b]			37.68			
Protein yield MGPGL(mg total protein/g of liver)[c]			120			
IVIVE $CL_{h,s,in}$ assuming 100% plasma membrane abundance (ml/min) (Eq. 6-8)	224±81	116±44	139±55	285±109	284±111	168±64
IVIVE $CL_{h,s,in}$ based on the WSHM and assuming 100% plasma membrane abundance (ml/min) (Eq. 5)	192±62	107±38	126±46	235±78	234±79	149±52
% plasma membrane abundance (%PMA)	36±2.5	64 ±9.3[a]	55±6.4[a]	52±11.5[a]	66±4.2[a]	59±6.7
IVIVE $CL_{h,s,in}$ (ml/min) corrected for OCT1 PMA (Eq. 6)	578±225	178±69	248±99	535±210	425±169	277±109
IVIVE $CL_{h,s,in}$ (ml/min) based on the WSHM and corrected for OCT1 PMA (Eq. 5)	405±122	157±56	208±74	382±119	323±105	230±78

a. OCT1 abundance and % PMA were obtained from our previous report (Kumar et al., 2019)

b. Each hepatic tissue (n=36) OCT1 total abundance and the corresponding protein yield MGMPGL were obtained from our previous report (Wang et al., 2016)

DMD Fast Forward. Published on August 25, 2020 as DOI: 10.1124/dmd.120.000156
This article has not been copyedited and formatted. The final version may differ from this version.

c. Value for the yield of total mg protein per gram of liver was obtained based on hypocellularity and total protein per million hepatocytes (Jones et al., 2012; Kim et al., 2019)

DMD Fast Forward. Published on August 25, 2020 as DOI: 10.1124/dmd.120.000156
This article has not been copyedited and formatted. The final version may differ from this version.

DMD Fast Forward. Published on August 25, 2020 as DOI: 10.1124/dmd.120.000156
This article has not been copyedited and formatted. The final version may differ from this version.

Figure 1

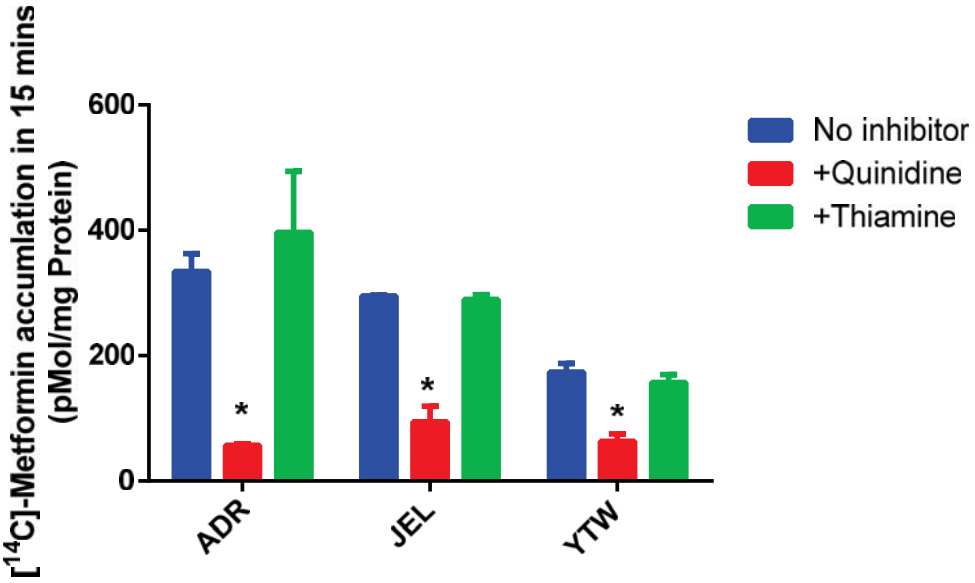

DMD Fast Forward. Published on August 25, 2020 as DOI: 10.1124/dmd.120.000156
This article has not been copyedited and formatted. The final version may differ from this version.

Figure 2

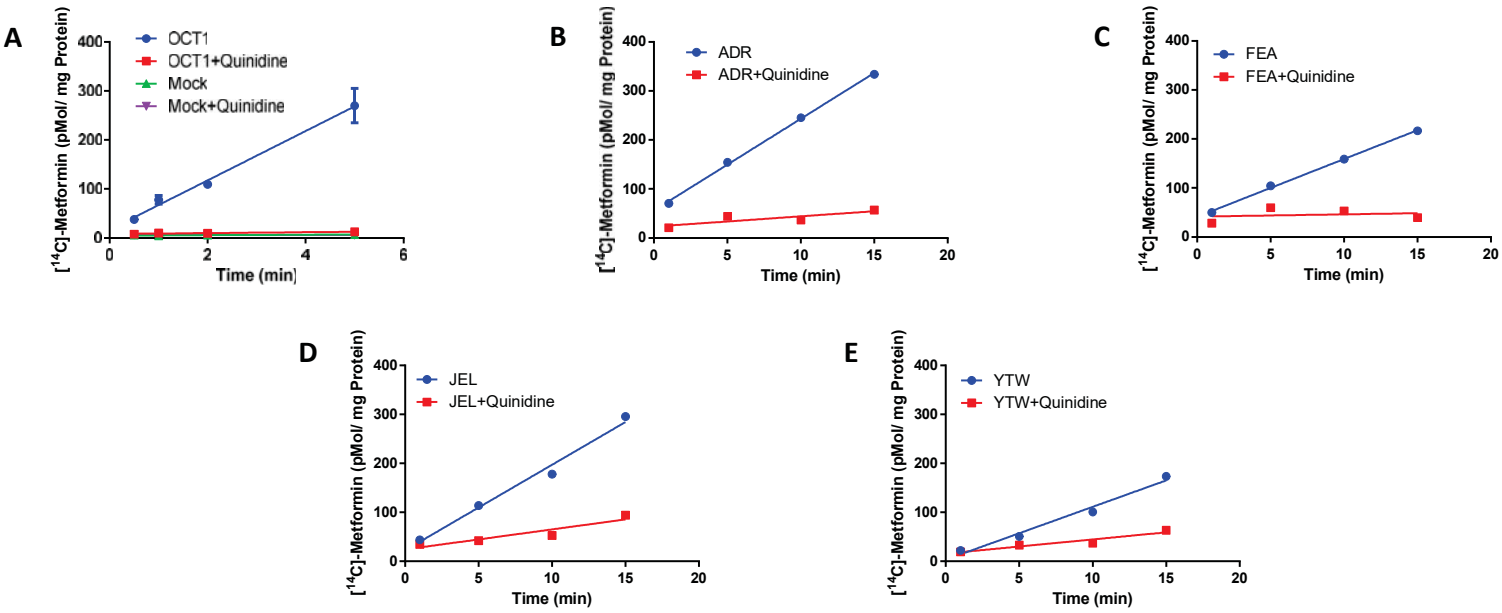

Figure 3

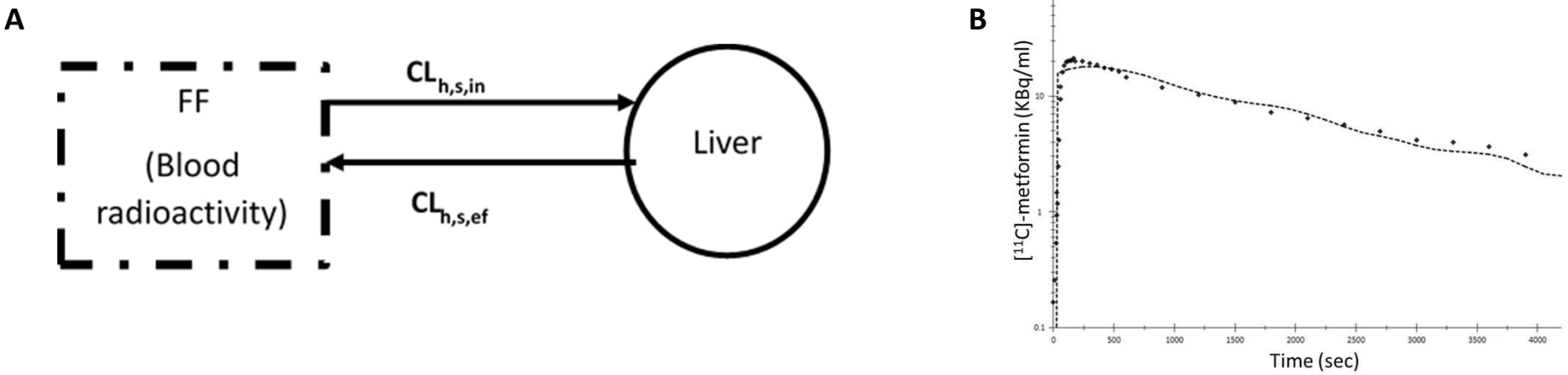

DMD Fast Forward. Published on August 25, 2020 as DOI: 10.1124/dmd.120.000156
This article has not been copyedited and formatted. The final version may differ from this version.

Figure 4